NAA-SR-8171
COPY

CORRELATION OF LIQUID FRACTION IN TWO-PHASE FLOW WITH APPLICATION TO LIQUID METALS

AEC Research and Development Report

ATOMICS INTERNATIONAL
A DIVISION OF NORTH AMERICAN AVIATION, INC.

DISCLAIMER

Price $1.00
Available from the Office of Technical Services
Department of Commerce
Washington 25, D. C.

NAA-SR-8171
REACTOR TECHNOLOGY
42 PAGES

CORRELATION OF LIQUID FRACTION IN TWO-PHASE FLOW WITH APPLICATION TO LIQUID METALS

AEC Research and Development Report

By
C. J. BAROCZY

ATOMICS INTERNATIONAL

A DIVISION OF NORTH AMERICAN AVIATION, INC.
P.O. BOX 309 CANOGA PARK, CALIFORNIA

CONTRACT: AT(11-1)-GEN-8
ISSUED: APR 15 1963

DISTRIBUTION

This report has been distributed according to the category "Reactor Technology" as given in "Standard Distribution Lists for Unclassified Scientific and Technical Reports," TID 4500 (19th Ed.), February 1, 1963. A total of 650 copies was printed.

CONTENTS

		Page
	Abstract	v
I.	Introduction	1
II.	Method of Correlation	3
	A. Two-Phase, Two-Component Liquid Fraction Data	3
	B. Generalized Liquid Fraction	8
III.	Comparison of Experimental and Predicted Liquid Fraction	13
IV.	Application of Correlation to Boiling Mercury	20
	Nomenclature	33
	References	35

TABLES

I.	Coordinates for Generalized Liquid Fraction Correlation	11

FIGURES

1.	Liquid Fraction vs X_{tt} and X_{vt} for Water-Air and Mercury-Nitrogen	4
2.	Liquid Fraction vs X_{tt} for Three Values of $\left(\frac{\mu_\ell}{\mu_g}\right)^{0.2} \Big/ \left(\frac{\rho_\ell}{\rho_g}\right)$	7
3.	Generalized Liquid Fraction Correlation	9
4.	Comparison of Martinelli-Nelson Correlation for Steam With Generalized Correlation	14
5.	Comparison of Experimental Void Fraction Data for Steam (Without Heat Addition) With Generalized Correlation	15

FIGURES

		Page
6.	Comparison of Experimental Void Fraction Data for Steam (115 psia) With Generalized Correlation	16
7.	Comparison of Experimental Void Fraction Data for Steam (614 psia) With Generalized Correlation	17
8.	Comparison of Experimental Void Fraction Data With Steam (2000 psia) With Generalized Correlation	18
9.	Comparison of Experimental Void Fraction Data for Santowax R With Generalized Correlation	19
10	Liquid Fraction vs X_{tt} for Mercury	22
11.	Liquid Fraction vs Relative Location in Boiling Length for Mercury With Uniform Heat Flux	24
12.	Length-Average Liquid Fraction vs Exit Quality for Boiling Mercury With Uniform Heat Flux	25
13.	Length-Average Mixture Density vs Exit Quality for Boiling Mercury With Uniform Heat Flux	27
14.	Slip Ratio vs Relative Location in Boiling Length for Mercury With Uniform Heat Flux	29
15.	Multiplier r vs Temperature for Mercury	32

ABSTRACT

This report presents a generalized correlation for liquid fraction in two-phase flow which is proposed for use with all fluids, including liquid metals. The correlation is based on isothermal, two-phase, two-component liquid fraction data for liquid mercury-nitrogen and water-air. Liquid fraction is shown to be a function of the Martinelli flow modulus and liquid/gas density and viscosity ratios. Good correspondence is indicated between the liquid fraction predicted by this correlation and the Martinelli-Nelson correlation for steam, experimental data for steam, and experimental data for Santowax R, an organic coolant. Prediction of liquid fraction by this method is shown for sodium, potassium, rubidium, and mercury. Application of the method to boiling mercury, for a range of temperatures and exit qualities, is demonstrated for SNAP systems.

ACKNOWLEDGMENT

The author thanks Paul D. Cohn for his encouragement, and Louis Bernath for his encouraging and valuable suggestions.

I. INTRODUCTION

In the co-current flow of liquid and gas (or vapor) in a pipe, the fraction of total flow area occupied by the liquid, i.e., the liquid fraction, bears strongly on the heat transfer and fluid flow characteristics of the system. Except for the condition where the densities of the phases are equal, the velocities of the phases are different; therefore, liquid fraction cannot be calculated directly from knowledge of the densities and weight flow rates of the respective phases. Consequently, liquid fraction in two-phase flow usually is determined experimentally, and then correlated by suitable means.

Of the many methods available for predicting liquid fraction, one of the earliest was that proposed by Martinelli, et al.[1] in which a wide range of two-phase, two-component liquid fraction data, for air and various liquids, were successfully correlated. Later, Lockhart and Martinelli[2] generalized the work performed previously;[1] the resultant correlation has become the most widely accepted method of predicting liquid fraction in two-phase flow.

Although generally successful in predicting liquid fraction within satisfactory limits, and major trends correctly, the Lockhart-Martinelli correlation has shortcomings. Martinelli-Nelson[3] found that a family of liquid fraction curves was required for steam, with saturation pressure as parameter, to correctly predict slip ratio near the critical point instead of the single curve proposed by Lockhart-Martinelli. Hughmark and Pressburg[4] showed that liquid fraction, for a number of liquid and gas combinations, depended on total mass velocity in addition to the Martinelli flow modulus. Sher[5] modified the Martinelli-Nelson liquid fraction curves, for steam at low qualities, to preclude slip ratios less than one.

Recently, analytical treatments have been made of two-phase pressure drop and liquid fraction. The Bankoff Model[6] has been used successfully for steam-water mixtures but requires modification for use with other fluid combinations. Levy's Model[7] has been applied successfully to steam-water mixtures and water-air mixtures. An empirical equation, involving fluid properties, was developed by von Glahn[8] for prediction of liquid fraction in steam-water mixtures. The Martinelli correlations[2,3] compare favorably with the liquid fraction predicted by each of the above methods. In total, the Martinelli form of correlation, with its limitations, satisfactorily predicts liquid fraction in

two-phase flow for a wide range of conditions far more often than it does not. The present correlation uses the Martinelli flow modulus and an additional parameter involving liquid/gas density and viscosity ratios.

Prediction of liquid fraction in industrial processes utilizing two-phase flow is of importance but generally is not critical to system performance. This is not so when boiling-fluid reactors or nuclear powered space systems, utilizing a boiler and condenser, are considered. Here accurate prediction of liquid fraction is required to attain system performance, reliability, and weight objectives. Although considerable liquid fraction data and many correlations are available for water and other commonly used fluids, virtually no data exist for liquid metals. Extrapolation of present correlations, which are based primarily on water, is difficult because the physical properties of liquid metals differ markedly from those of water. For a given temperature, the most striking difference is the prevalence of extremely high liquid/gas density ratios for liquid metals.

A convenient method of obtaining liquid hold-up data involving high liquid/gas density ratios and utilizing a liquid metal, is the use of liquid mercury-nitrogen in an isothermal, two-phase, two-component test. Such experimental data were obtained[9] to provide a basis for analysis and performance prediction for the SNAP 2, nuclear-powered, Rankine cycle space system.[10]

The present correlation is based on liquid mercury-nitrogen data[9] and water-air data.[11,12] The liquid/gas density ratios for these data are 9350 and 665, respectively. Since the present correlation is of a generalized form, and the properties variation range described above encompasses that for liquid metals, it is proposed that the correlation be used in predicting liquid fraction for liquid metals. While verification of the correlation with single component liquid metals was not possible, because of a lack of data, good agreement was obtained for a variety of two-component and single component liquid fraction data.

II. METHOD OF CORRELATION

A. TWO-PHASE, TWO-COMPONENT LIQUID FRACTION DATA

The experimental liquid fraction data which served as the basis for the generalized correlation is illustrated in Figure 1. Shown is the correlation for water-air by Hewitt, et al.[11,12] and the present correlation for liquid mercury-nitrogen based on the data of Koestel and Kiraly.[9] Each of the above correlations shows two distinct curves when R_ℓ, the liquid fraction, is plotted against the Martinelli flow moduli, X_{vt} and X_{tt}.[2]

From [2] the flow modulus X is defined as,

$$X = \left[\frac{\left(\frac{\Delta P}{\Delta L}\right)_\ell}{\left(\frac{\Delta P}{\Delta L}\right)_g}\right]^{\frac{1}{2}} , \qquad (1)$$

where $\left(\frac{\Delta P}{\Delta L}\right)_\ell$ and $\left(\frac{\Delta P}{\Delta L}\right)_g$ are the pressure drop gradients for liquid flowing only and gas flowing only, respectively. For the viscous liquid-turbulent gas flow regime

$$X_{vt} = \left[\frac{C_\ell}{C_g}\,\frac{\rho_g}{\rho_\ell}\,\frac{\mu_\ell}{\mu_g}\,\frac{W_\ell}{W_g}\right]^{0.5} \frac{1}{\left(N_R\right)_g^{0.4}} , \qquad (2)$$

where C is a constant in the Fanning friction pressure drop expression, ρ is density, μ is absolute viscosity, W is weight flow rate, and N_R is Reynolds number. The subscripts ℓ and g refer to the liquid and gas phases,* respectively. A Reynolds number of 2000 or more, for each phase flowing alone, indicates turbulent flow; less than 2000, viscous flow.

---

* The terms "gas" and "vapor" are used synonymously.

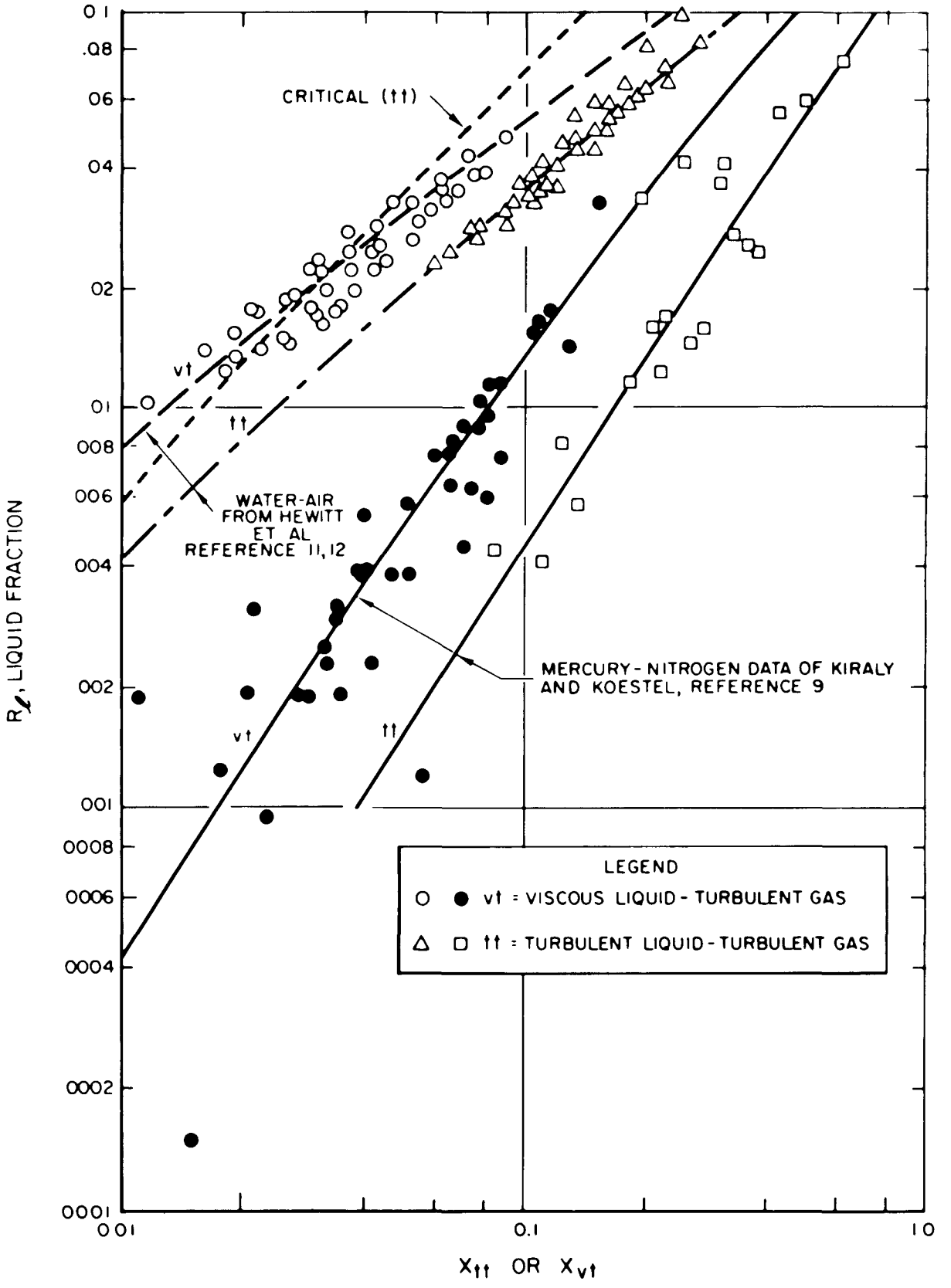

Figure 1. Liquid Fraction vs X_{tt} and X_{vt} for Water-Air and Mercury-Nitrogen

Similarly, for the turbulent liquid-turbulent gas flow regime,

$$X_{tt} = \left(\frac{W_\ell}{W_g}\right)^{0.9} \left(\frac{\rho_g}{\rho_\ell}\right)^{0.5} \left(\frac{\mu_\ell}{\mu_g}\right)^{0.1} \quad . \tag{3}$$

R_ℓ, the liquid fraction, is defined as the fraction of pipe cross section occupied by liquid in co-current liquid-gas flow. Similarly, R_g is the fraction of pipe cross section occupied by gas in co-current liquid-gas flow, and is equal to $1 - R_\ell$. Terms are defined in the Nomenclature Section p 33.

The water-air data of Hewitt, et al.[11,12] were obtained using vertical up-flow in 1.25-in. diameter tube. The annular flow pattern prevailed in all tests. In Reference 11 the liquid hold-up was obtained by trapping the liquid-gas mixture in the test section and weighing the liquid; in Reference 12 the liquid hold-up was obtained by measuring the liquid film thickness. It can be seen that two distinct curves are indicated by the data with R_ℓ, the liquid fraction, being about one and one-half times greater for the vt flow regime than for the tt flow regime. The vt flow regime curve also corresponds to the Lockhart-Martinelli curve which was advanced as being independent of flow regime, i.e., the single curve for R_ℓ is valid for all combinations of viscous and turbulent flow for each component. The Lockhart-Martinelli curve is based on data obtained earlier by Martinelli, et al.[1] for a variety of fluid combinations flowing in horizontal tubes. These data include not only the annular flow pattern, but a variety (see References 1 for descriptions) of other commonly observed flow patterns. Thus the total effect of different flow patterns is implicit in the Lockhart-Martinelli curve and the good agreement with the data of Hewitt et al., for annular flow only, indicates that satisfactory prediction of liquid fraction in isothermal, two-phase flow is possible without detailed knowledge of flow pattern. An apparently similar independence of two-phase pressure drop on knowledge of flow pattern was demonstrated by Lockhart-Martinelli.[2] More detailed information on the influence of flow pattern on two-phase pressure drop and liquid fraction is contained in the survey made by Vohr.[13]

The two-lower curves in Figure 1 represent the best fit correlation of liquid fraction for mercury-nitrogen based on the data of Kiraly and Koestel.[9*]

---

* The two-phase, two-component pressure drop data of this experiment were previously correlated by Baroczy and Sanders.[14]

The test section consisted of a 0.394-in. diameter, horizontal glass tube. The liquid hold-up was obtained by trapping the liquid-gas mixture in the test section, using solenoid valves, and then measuring the liquid volume. It can be seen that approximately three times greater liquid fraction is indicated for the vt flow regime than for the tt flow regime. This is similar to the pattern shown by Hewitt, et al.[11,12] for water-air. Comparison shows that the experimental liquid fraction for liquid mercury-nitrogen is on the order of 10% of that predicted by the Lockhart-Martinelli curve. As in the case of the liquid fraction data of,[1] the liquid mercury-nitrogen data encompass a variety of flow patterns (described in Reference 9) and inherently reflect their effect. Since the tt region generally applies to boiling processes and permits the calculation of an additional liquid fraction curve, as explained below, it was chosen for the correlation. Figure 2 shows R_ℓ, the liquid fraction, as a function of X_{tt} for the water-air data[11,12] and the liquid mercury-nitrogen data.[9] The liquid/gas density ratio for water-air was 665; for liquid mercury-nitrogen, 9350. It is proposed that the displacement in the curves is due to primarily liquid/gas density ratio, and secondarily, liquid/gas viscosity ratio. A somewhat similar pattern was shown, for steam only, by Martinelli-Nelson[3] in which saturation pressure served as the parameter. Here it is proposed that liquid fraction can be predicted for any fluid combination when R_ℓ is plotted against X_{tt} with $\left(\frac{\mu_\ell}{\mu_g}\right)^{0.2} \Big/ \left(\frac{\rho_\ell}{\rho_g}\right)$ as a parameter. Since $\left(\frac{\mu_\ell}{\mu_g}\right)$ and $\left(\frac{\rho_\ell}{\rho_g}\right)$ appear in X_{tt}, it appears possible to express R_ℓ in the form of a single equation.

To establish an upper limit curve, the liquid fraction for the two-component critical condition* was calculated in the manner suggested by Martinelli-Nelson.[3] Using Equation 3 for the condition where the density and viscosity ratios are equal, and the relationship that gas fraction, R_g, is equal to the ratio of gas to total weight flow, resulted in the upper liquid fraction curve shown in Figure 2 and Figure 1.

---

* While strictly appropriate for a single component, it may be reasoned that it is also valid, as a limiting case, for two-component flow for the condition where the liquid and gas densities, and viscosities, are equal.

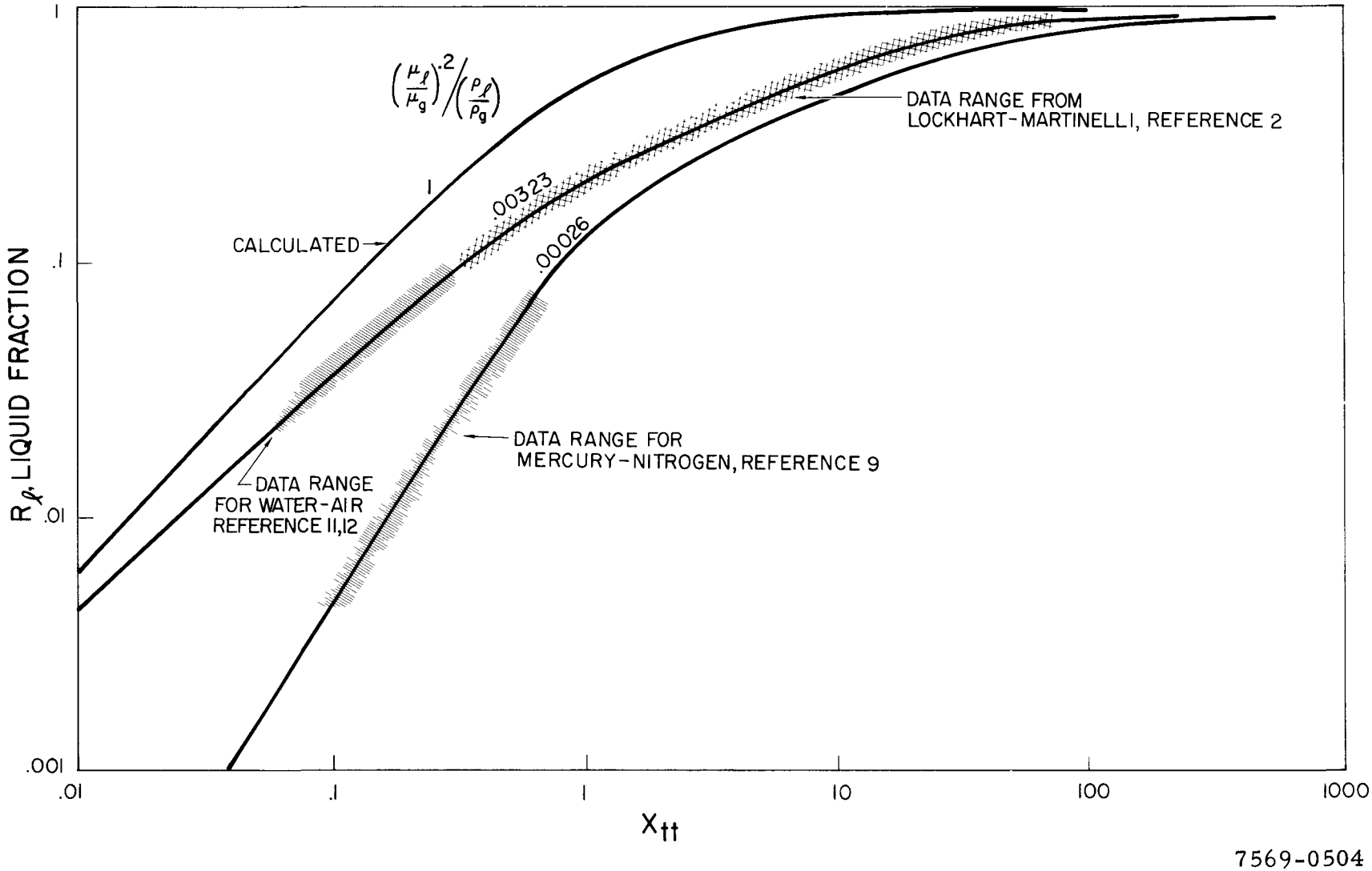

Figure 2. Liquid Fraction vs X_{tt} for Three Values of $\left(\frac{\mu_\ell}{\mu_g}\right)^{0.2}\Big/\left(\frac{\rho_\ell}{\rho_g}\right)$

Thus, three curves are shown in which the parameter $\left(\frac{\mu_\ell}{\mu_g}\right)^{0.2}\Big/\left(\frac{\rho_\ell}{\rho_g}\right)$ has the values 1, 0.00323, and 0.00026, for the two-component critical condition, water-air, and liquid mercury-nitrogen, respectively. The shaded area shows the range of the present data while the cross-hatched area shows the range of the Lockhart-Martinelli data.[2] The liquid fraction data of Chisholm and Laird[15] for water-air flow in a smooth tube generally fall slightly below the cross-hatched area. The liquid fraction data of Richardson[16] for water-air flow in smooth rectangular flow sections generally fall into the cross-hatched area.

Extrapolation of the curves beyond the range covered by the present data was achieved by assuming a slip ratio* of one for extremely high liquid/gas weight flow ratios (10,000 for water-air; 100,000 for liquid mercury-nitrogen), and calculating the corresponding liquid fraction for each fluid combination. The Lockhart-Martinelli curve was then used as a guide in establishing the shape of the curves between the limit of the present data, and the points calculated above. Each of the three curves shows that as X_{tt} increases, R_ℓ increases rapidly, initially, and then at a slower rate. At very high values of X_{tt} (corresponding to high liquid/gas weight flow ratios), R_ℓ for all curves approaches one.

A similar generalized correlation for the vt flow regime was not attempted as a family of two-component critical curves results, with gas Reynolds number as a parameter, instead of the single curve for the tt flow regime.

B. GENERALIZED LIQUID FRACTION

By cross-plotting the curves in Figure 2, the generalized correlation of Figure 3 was obtained showing R_ℓ as a function of $\left(\frac{\mu_\ell}{\mu_g}\right)^{0.2}\Big/\left(\frac{\rho_\ell}{\rho_g}\right)$ and X_{tt}. For given value of X_{tt} liquid fraction increases quite rapidly up to $\left(\frac{\mu_\ell}{\mu_g}\right)^{0.2}\Big/\left(\frac{\rho_\ell}{\rho_g}\right)$

* See Section IV for derivation of slip ratio expression.

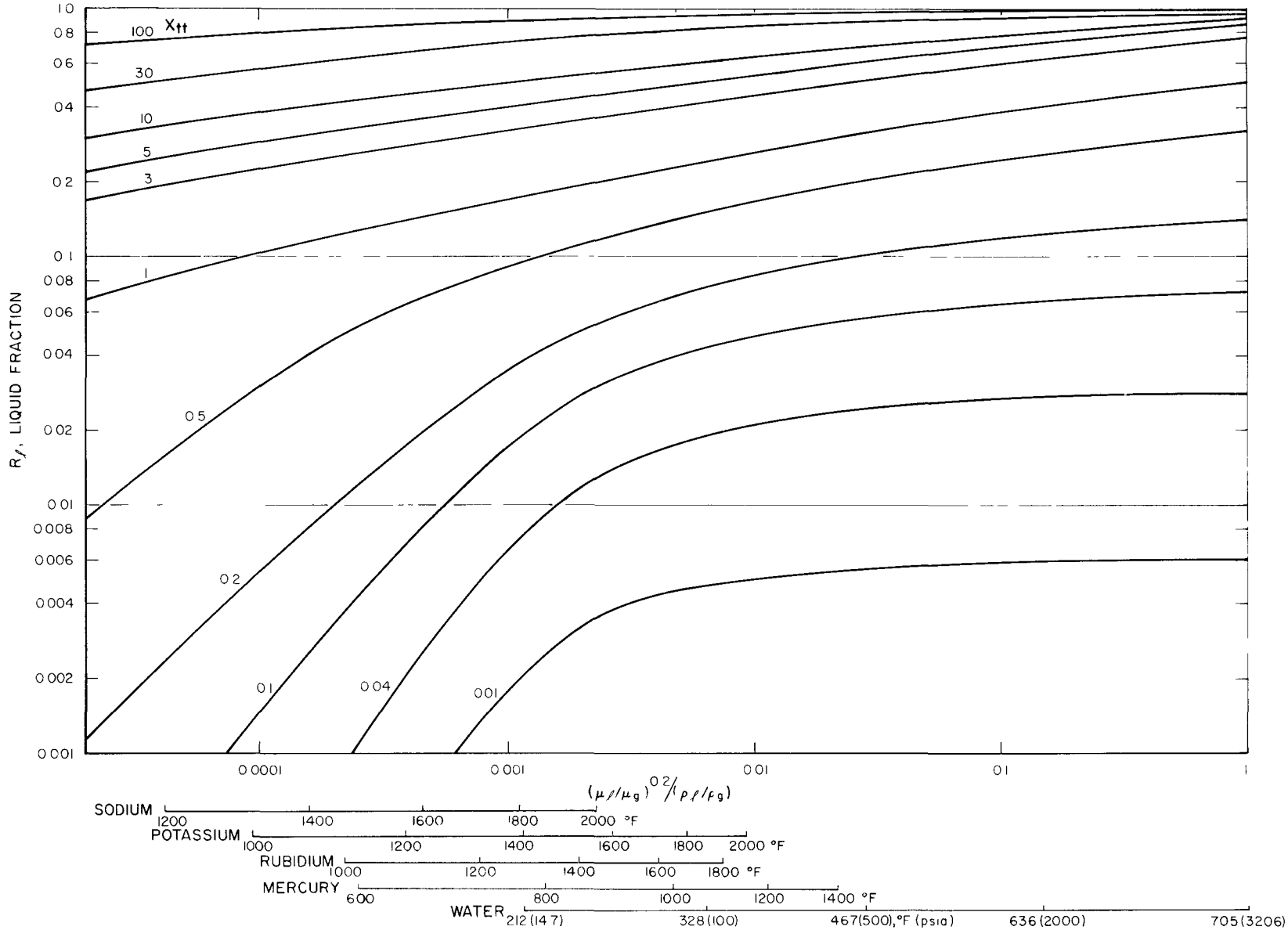

7569-0505

Figure 3. Generalized Liquid Fraction Correlation

equal to about 0.01; beyond this the rate decreases considerably. As X_{tt} increases, the liquid fraction curves become flatter for all values of the parameter $\left(\frac{\mu_\ell}{\mu_g}\right)^{0.2} \Big/ \left(\frac{\rho_\ell}{\rho_g}\right)$.

It is emphasized that each of the curves shown in Figure 3 is based on only three points, as obtained from Figure 2. The shapes of the curves resulted from appropriate fairing between the points and, to cover the range shown, additionally reflect extrapolation below

$$\left(\frac{\mu_\ell}{\mu_g}\right)^{0.2} \Big/ \left(\frac{\rho_\ell}{\rho_g}\right) \quad ,$$

values less than 0.00026, and X_{tt} values less than 0.05. Confirmation of the correlation will require the accumulation of substantial amounts of two-phase, single-component liquid fraction data. Until such time, the correlation is proposed for use with liquid metals as it is of a generalized form and affords good agreement with a variety of experimental liquid fraction data.

For comparative purposes the relative positions of sodium, potassium, rubidium, mercury, and water are shown at various saturation temperatures. The appropriate liquid metal properties are from Weatherford, et al.[17] It can be seen that liquid fraction for the liquid metals generally corresponds to that of low pressure (less than 100 psia) steam. For convenience, the coordinates of Figure 3 are plotted in Table I for both the generalized correlation and the liquid metals.

TABLE I

COORDINATES FOR GENERALIZED LIQUID FRACTION CORRELATION

R_ℓ, Liquid Fraction

$\left(\frac{\mu_\ell}{\mu_g}\right)^{0.2}\left(\frac{\rho_\ell}{\rho_g}\right)$	X_{tt}										
	0.01	0.04	0.1	0.2	0.5	1	3	5	10	30	100
0.00002				0.0012	0.009	0.068	0.17	0.22	0.30	0.47	0.71
0.0001			0.0015	0.0054	0.030	0.104	0.23	0.29	0.38	0.57	0.79
0.0004		0.0022	0.0072	0.0180	0.066	0.142	0.28	0.35	0.45	0.67	0.85
0.001	0.0018	0.0066	0.0170	0.0345	0.091	0.170	0.32	0.40	0.50	0.72	0.88
0.004	0.0043	0.0165	0.0370	0.0650	0.134	0.222	0.39	0.48	0.58	0.80	0.92
0.01	0.0050	0.0210	0.0475	0.0840	0.165	0.262	0.44	0.53	0.63	0.84	0.94
0.04	0.0056	0.0250	0.0590	0.1050	0.215	0.330	0.53	0.63	0.72	0.90	0.96
0.10	0.0058	0.0268	0.0640	0.1170	0.242	0.380	0.60	0.70	0.78	0.92	0.98
1.0	0.0060	0.0280	0.0720	0.1400	0.320	0.500	0.75	0.85	0.90	0.94	0.994

R_ℓ, Liquid Fraction

Sodium											
1200°F				0.0023	0.016	0.082	0.192	0.25	0.33	0.51	0.75
1400			0.0025	0.0082	0.041	0.116	0.242	0.31	0.40	0.60	0.81
1600		0.0025	0.0080	0.0193	0.069	0.145	0.285	0.36	0.46	0.67	0.86
1800	0.0020	0.0072	0.0185	0.0370	0.094	0.174	0.325	0.40	0.50	0.73	0.88
2000	0.0035	0.0127	0.0295	0.0530	0.117	0.200	0.360	0.44	0.55	0.77	0.90

TABLE I (Cont.)

COORDINATES FOR GENERALIZED LIQUID FRACTION CORRELATION

	R_ℓ, Liquid Fraction										
Potassium	0.01	0.04	0.1	0.2	0.5	1	3	5	10	30	100= X_{tt}
1000°F			0.0014	0.005	0.028	0.102	0.22	0.28	0.37	0.56	0.79
1200		0.0020	0.0068	0.017	0.065	0.140	0.28	0.35	0.45	0.66	0.85
1400	0.0020	0.0075	0.0190	0.038	0.095	0.175	0.32	0.40	0.51	0.73	0.88
1600	0.0038	0.0140	0.0318	0.057	0.120	0.205	0.37	0.45	0.56	0.78	0.91
1800	0.0046	0.0181	0.0410	0.071	0.144	0.235	0.40	0.41	0.60	0.81	0.92
2000	0.0050	0.0205	0.0465	0.082	0.162	0.260	0.44	0.53	0.63	0.84	0.94
Rubidium											
1000			0.0037	0.011	0.050	0.12	0.25	0.32	0.42	0.62	0.83
1200	0.0013	0.0050	0.0138	0.029	0.084	0.16	0.31	0.39	0.48	0.71	0.88
1400	0.0032	0.0117	0.0272	0.050	0.111	0.20	0.35	0.44	0.54	0.76	0.90
1600	0.0044	0.0168	0.0375	0.066	0.135	0.22	0.39	0.48	0.58	0.80	0.92
1800	0.0048	0.0198	0.0445	0.078	0.156	0.25	0.42	0.51	0.62	0.83	0.94
Mercury											
600°F		0.0011	0.0043	0.012	0.05	0.13	0.26	0.33	0.42	0.63	0.83
800	0.0025	0.0090	0.0220	0.043	0.10	0.18	0.33	0.42	0.52	0.74	0.89
1000	0.0045	0.0175	0.0395	0.069	0.14	0.23	0.40	0.49	0.59	0.81	0.92
1200	0.0050	0.0212	0.0490	0.086	0.17	0.27	0.45	0.54	0.64	0.85	0.94
1400	0.0054	0.0235	0.0540	0.097	0.19	0.30	0.49	0.58	0.68	0.88	0.96

III. COMPARISON OF EXPERIMENTAL AND PREDICTED LIQUID FRACTION

To test the validity of the generalized correlation, it was compared to the Martinelli-Nelson correlation for steam;[3] the steam void fraction data of Isbin et al.,[17] Larson,[19] Marchaterre,[20] and Egen et al.;[21] and the void fraction data of Bergonzoli and Halfen,[22] for Santowax R.

Figure 4 shows that an agreement is generally obtained between the Martinelli-Nelson correlation for steam and the present correlation with the greatest difference occuring at atmospheric pressure. The difference arises from the Martinelli-Nelson assumption that the liquid fraction data of References 1 and 2 for water-air (liquid/gas density ratio about 600) would correspond to that of atmospheric pressure steam (liquid/gas density ratio of 1600). Since the present correlation takes into account the proper liquid/gas density and viscosity ratios, smaller liquid fraction is predicted by it than by the Martinelli-Nelson correlation.

Figure 5 shows the comparison between experimental void fraction data for steam, without heat addition, and the present correlation. The data of Isbin, et al.[18] at atmospheric pressure, and Larson[19] at 1000 psia, are shown to be in agreement with the correlation. Comparison of the correlation with the steam void fraction data of Marchaterre,[20] at 115 psia and 614 psia, is shown in Figures 6 and 7, and in Figure 8 for the data of Egen, et al.,[21] at 2000 psia. These data were obtained in a boiling system; here too, an agreement is indicated.

The void fraction data of Bergonzoli and Halfen,[22] obtained by boiling Santowax R, an organic coolant, were compared to the correlation and the result is shown in Figure 9. Very good agreement is shown as the average absolute deviation, for thirty-seven tests, is only about 7%. This is especially significant in that the parameter, $\left(\frac{\mu_\ell}{\mu_g}\right)^{0.2} \Big/ \left(\frac{\rho_\ell}{\rho_g}\right)$, for the Santowax R data was generally about four times greater than the data of Hewitt et al.[1,2] That is, the Santowax R test conditions were much closer to the critical point than the data used to develop the generalized correlation. The good agreement obtained between the correlation and the Santowax R data, and the 2000 psia steam data of

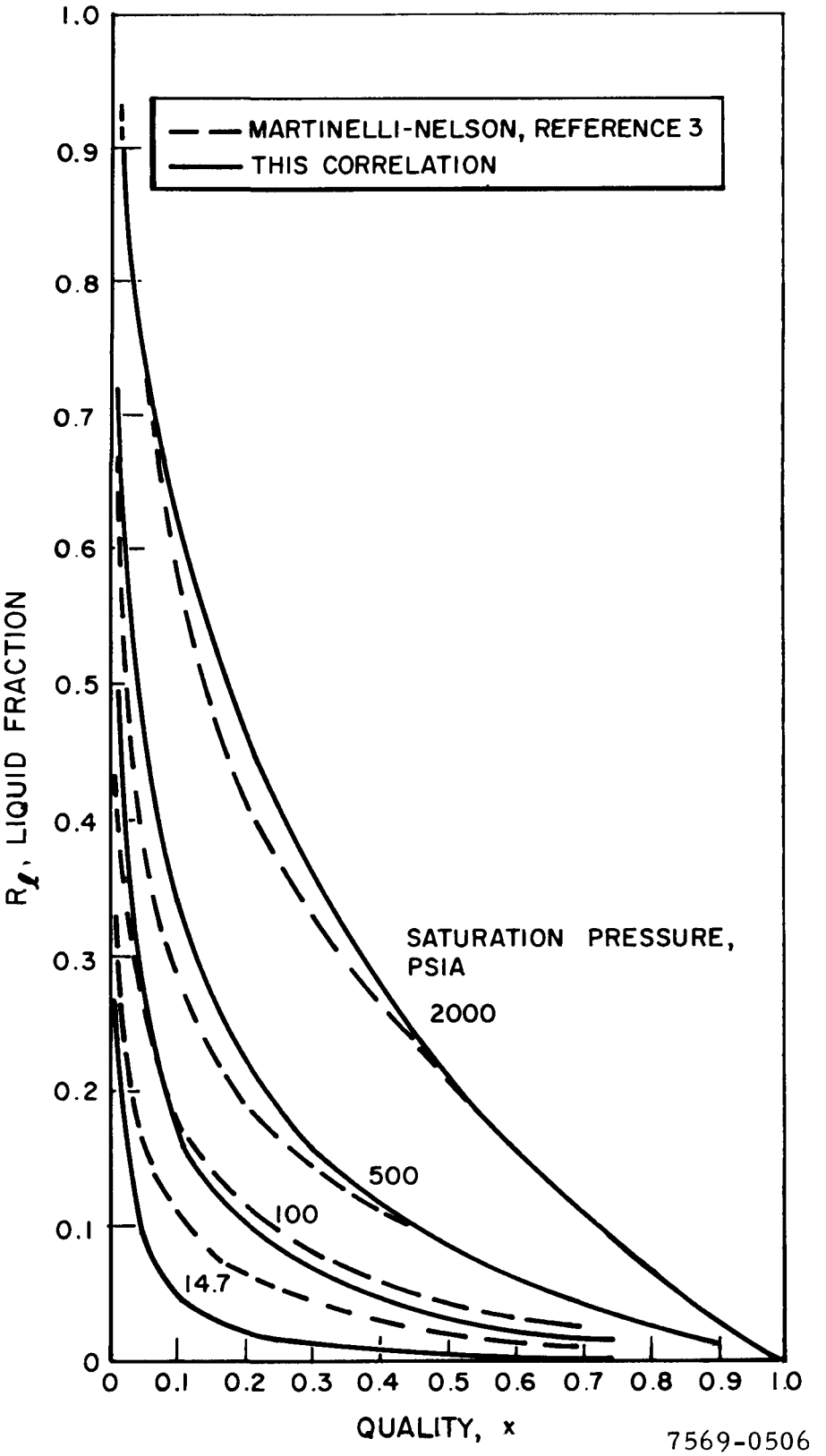

Figure 4. Comparison of Martinelli-Nelson Correlation for Steam With Generalized Correlation

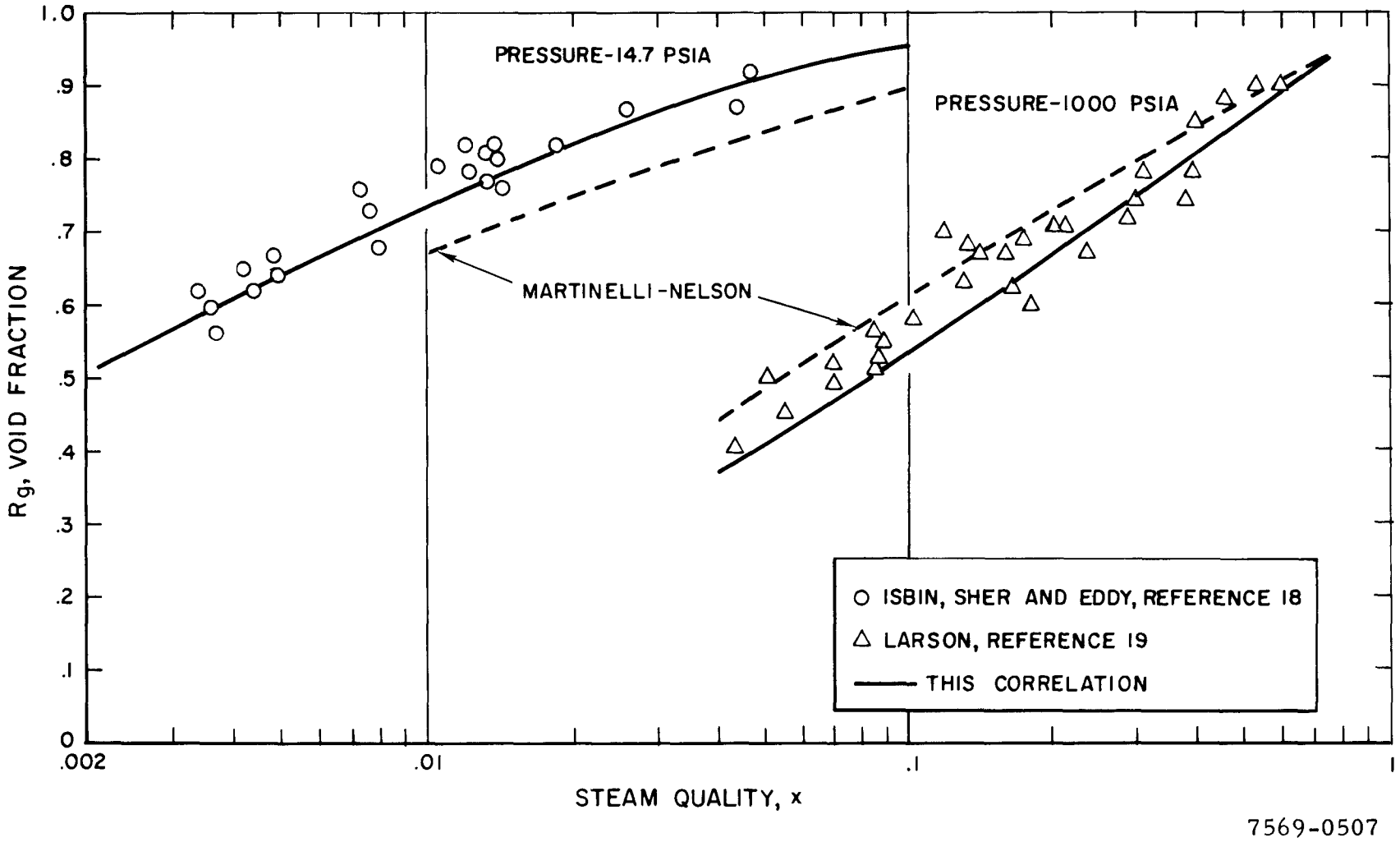

Figure 5. Comparison of Experimental Void Fraction Data for Steam (Without Heat Addition) With Generalized Correlation

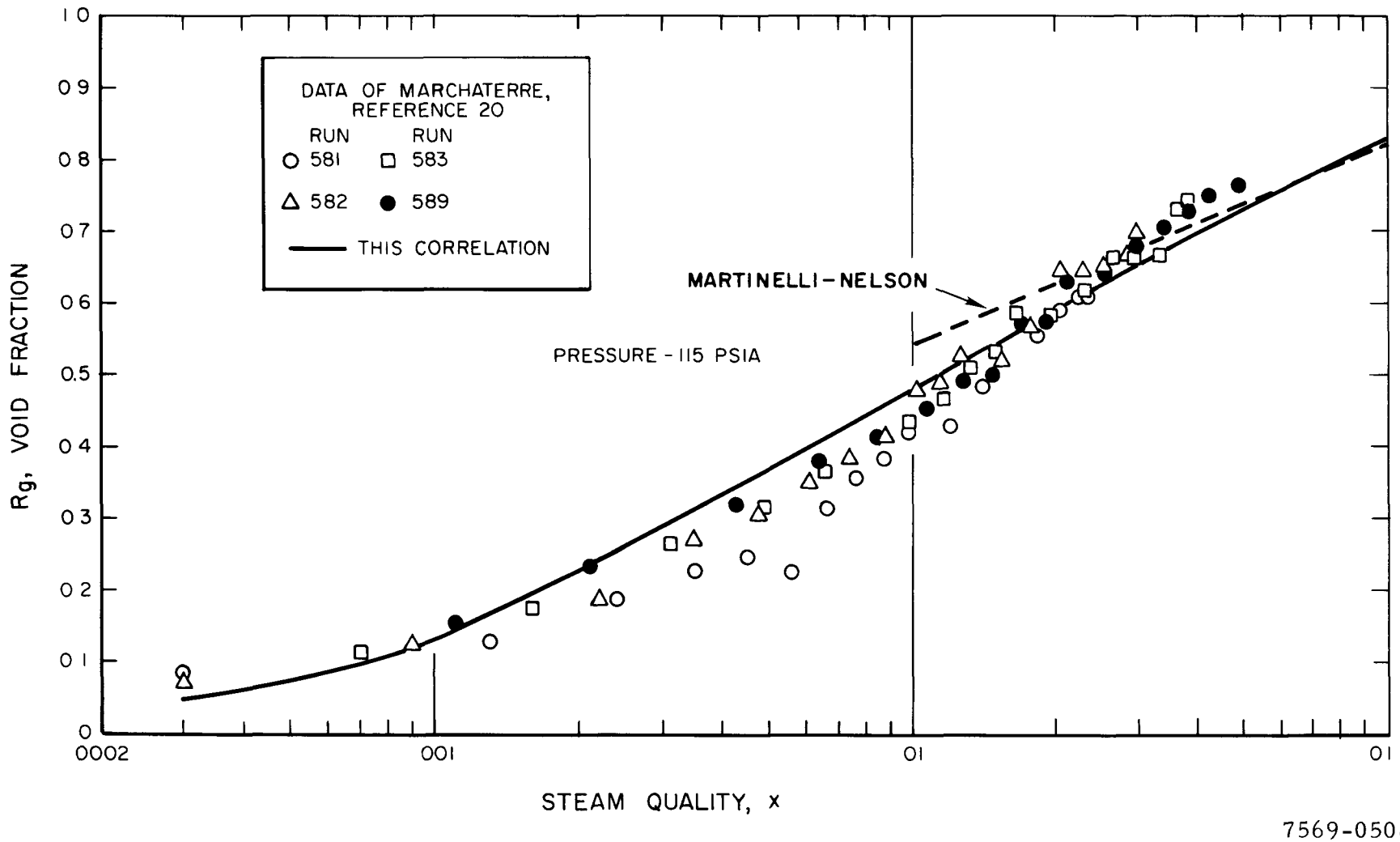

Figure 6. Comparison of Experimental Void Fraction Data for Steam (115 psia) With Generalized Correlation

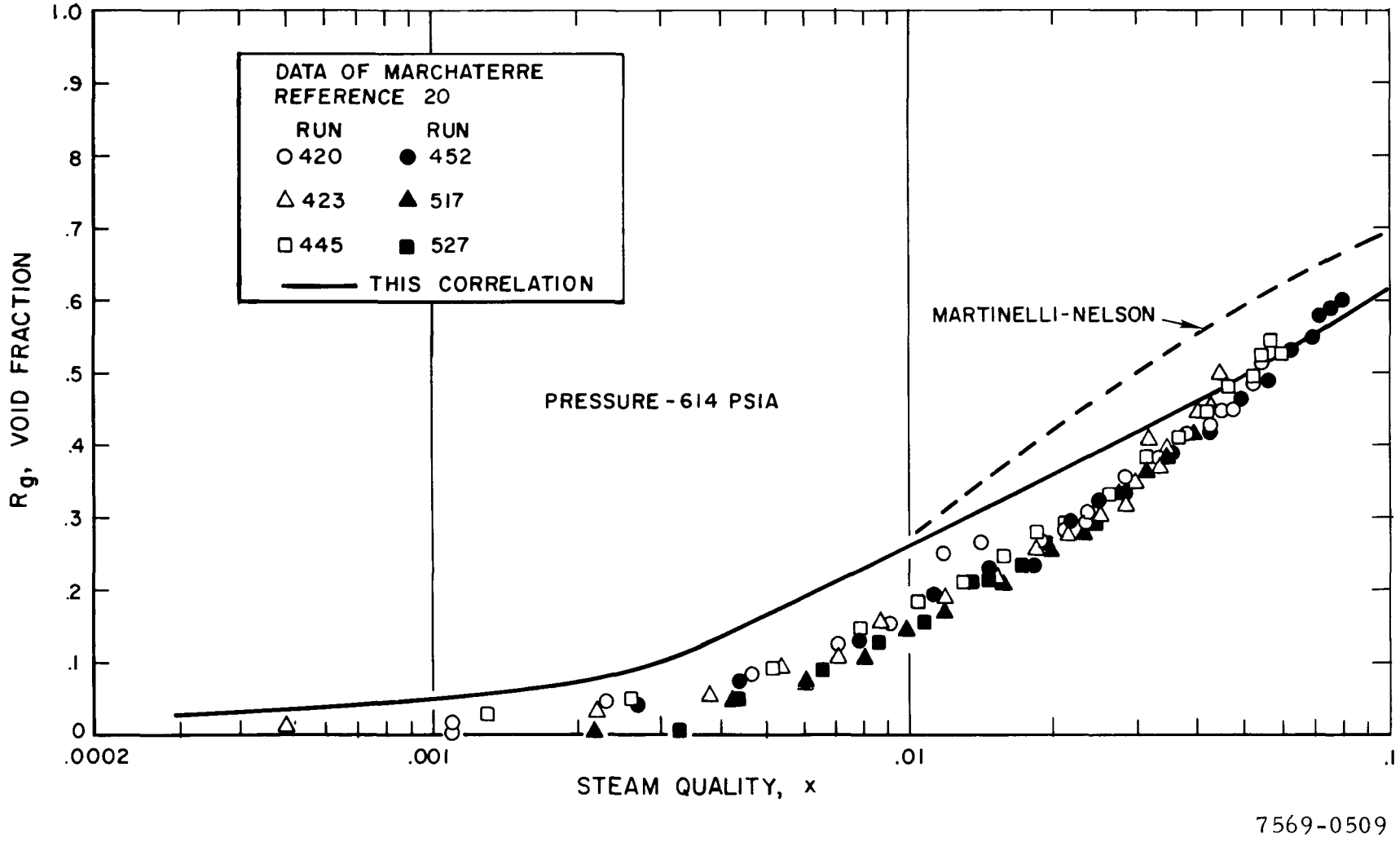

Figure 7. Comparison of Experimental Void Fraction Data for Steam (614 psia) With Generalized Correlation

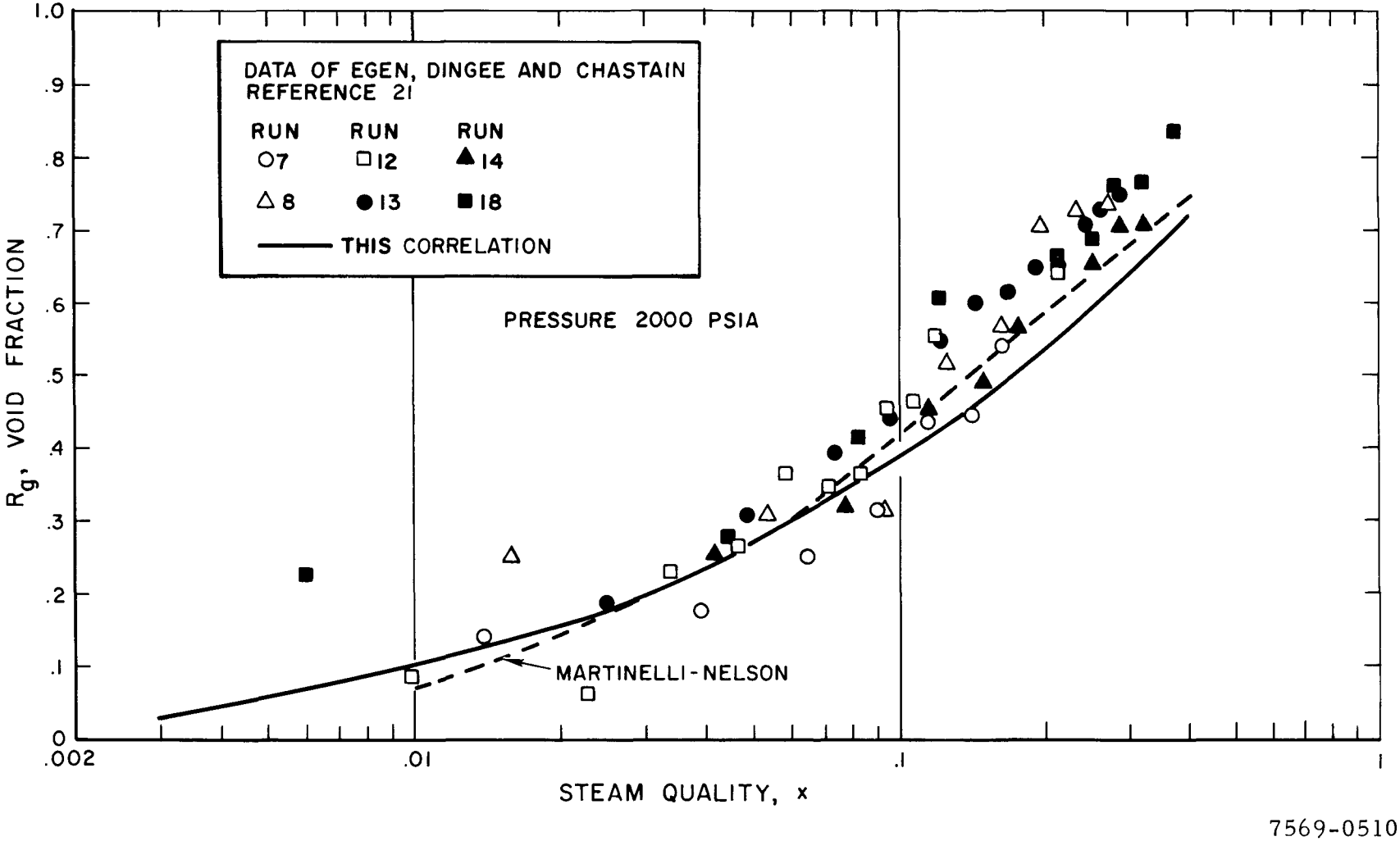

Figure 8. Comparison of Experimental Void Fraction Data With Steam (2000 psia) With Generalized Correlation

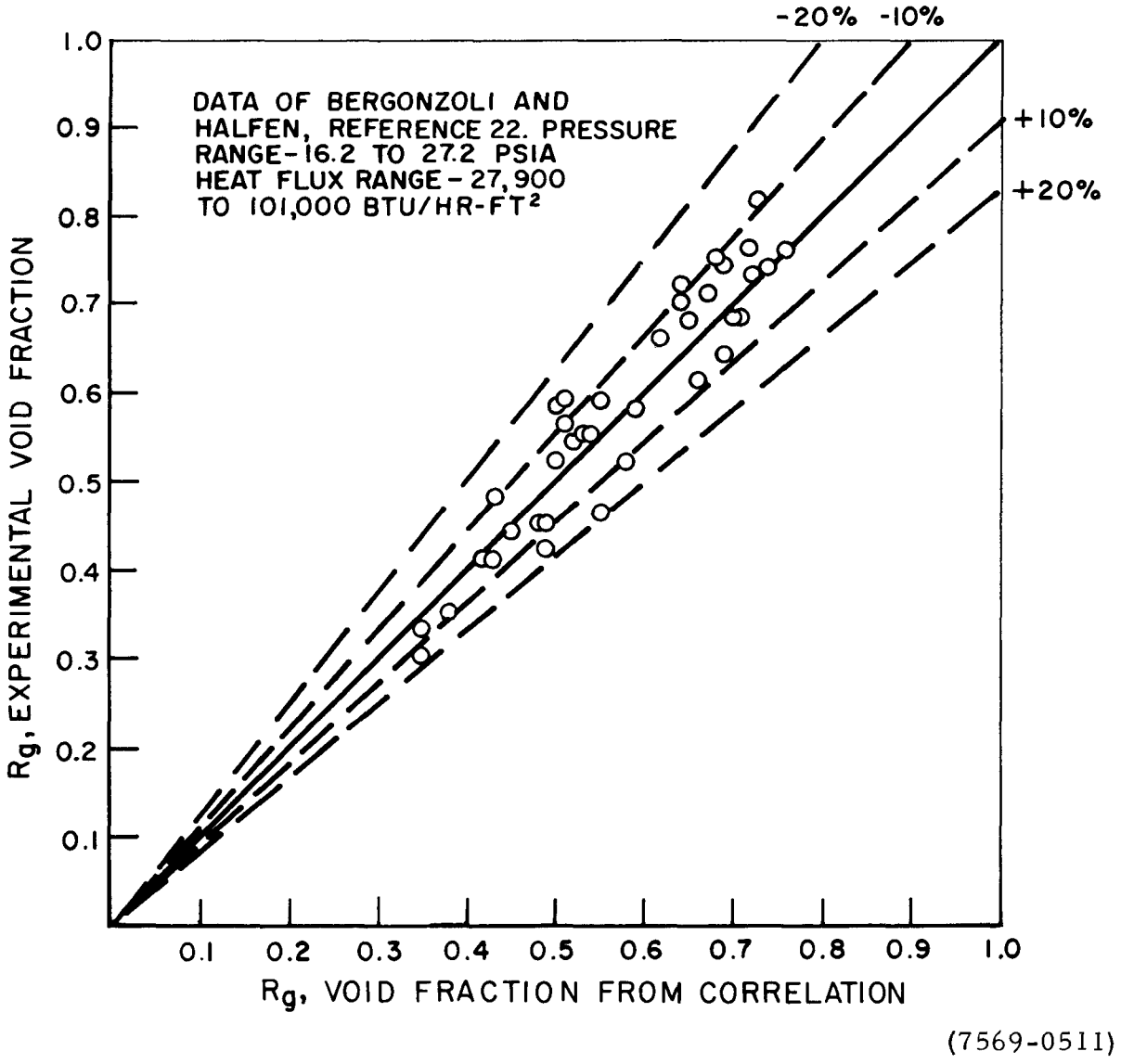

Figure 9. Comparison of Experimental Void Fraction Data for Santowax R With Generalized Correlation

Egen, et al.,[21] lends some support to the correctness of the liquid fraction curves in the region where the parameter, $\left(\frac{\mu_\ell}{\mu_g}\right)^{0.2} \Big/ \left(\frac{\rho_\ell}{\rho_g}\right)$, approaches 1.

IV. APPLICATION OF CORRELATION TO BOILING MERCURY

The use of mercury as the working fluid in nuclear space power systems, such as SNAP 2,[10] makes for particular interest. In addition, the very high density of liquid mercury (approximately 780 lb/cu ft) makes the prediction of working fluid inventory in two-phase components, such as boilers and condensers, of considerable importance. Thus the generalized correlation was utilized to predict the local liquid fraction, the length-average liquid fraction, the length-average mixture density, slip ratio, and the momentum pressure drop multiplier for boiling mercury at temperatures of 800 to 1400°F, and exit qualities of 0.1 to 1.

The system considered consists of a straight horizontal tube of uniform cross section into which there enters liquid at saturation conditions. The liquid and vapor content are in thermodynamic equilibrium and the heat of vaporization is constant. All heat transfer to the tube results in the formation of vapor and each phase, when flowing alone in the pipe, is in the turbulent condition (tt flow regime).* It is assumed that essentially static conditions exist at any point in the boiling length. This permits the use of two-phase, two-component liquid fraction data, as originally suggested by Martinelli-Nelson,[3] for single component flow in which a change of phase is occurring. The vapor flow rate W_g, at a point z in the boiling length is

$$W_g = \frac{P_w}{\lambda} \int_o^z \left(\frac{Q}{A_s}\right)\left(z'\right)\, dz' \qquad (4)$$

* Evidently the assumption of the tt flow regime existing everywhere in the boiling length is not valid at the all liquid entrance section and the vapor exit section for a quality of 1. However, the liquid fraction at these points is known to be one and zero, respectively. In addition, under certain conditions, there may be sections where the turbulent liquid-viscous gas flow regime (tv) may exist and other sections where the viscous liquid-turbulent gas flow regime (vt) may exist. Although dependent on flow rates, fluid properties, and system geometry, the tv flow regime is most likely to occur in the initial section of the boiling length while the vt flow regime is most likely to occur in latter portion of the boiling length. In boiling processes, the tv and vt flow regimes usually exist over small portions of the boiling length and, although data for these flow regimes is not included here, the liquid fraction can be estimated by interpolation between the known liquid fractions existing on either side of these areas.

where λ is the latent heat of vaporization, (Q/A_s) is the heat flux and is a function of z', and P_w is the wetted perimeter. For the case of uniform heat flux the vapor flow rate is proportional to the boiling length, or $W_g = Kz$. The vapor weight flow rate at the end of the boiling section is $(W_g)_o = KL = W_T x_o$. Combining these expressions results in

$$W_g = W_T x_o \left(\frac{z}{L}\right) \quad , \tag{5}$$

where W_T is the total flow rate, x_o is the exit quality, z is a point in the boiling section, and L is the boiling length. Since W_ℓ, the liquid flow rate, at any point is equal to $W_T - W_g$, the liquid/vapor flow rate ratio can be expressed as,

$$\frac{W_\ell}{W_g} = \frac{1}{x_o \left(\frac{z}{L}\right)} - 1 \quad . \tag{6}$$

Substituting the above expression into equation 3 results in,

$$X_{tt} = \left[\frac{1}{x_o \left(\frac{z}{L}\right)} - 1\right]^{0.9} \left(\frac{\rho_g}{\rho_\ell}\right)^{0.5} \left(\frac{\mu_\ell}{\mu_g}\right)^{0.1} \quad . \tag{7}$$

For any heat flux distribution other than the uniform case described above, the same method applies as long as $\frac{W_\ell}{W_g}$ can be expressed as a function of $\left(\frac{z}{L}\right)$.

Utilizing Table I, for mercury, Figure 10 was plotted showing R_ℓ as a function of X_{tt} for saturation temperatures of 600, 800, 1000, 1200, and 1400°F. By choosing values of $\left(\frac{z}{L}\right)$ from 0.001 to 1, and then using Equation 7, Figure 10, and the appropriate physical properties of mercury[17] for 800, 1000, 1200, and 1400°F, R_ℓ was obtained for exit qualities of 0.1, 0.3, 0.75, and 1. For

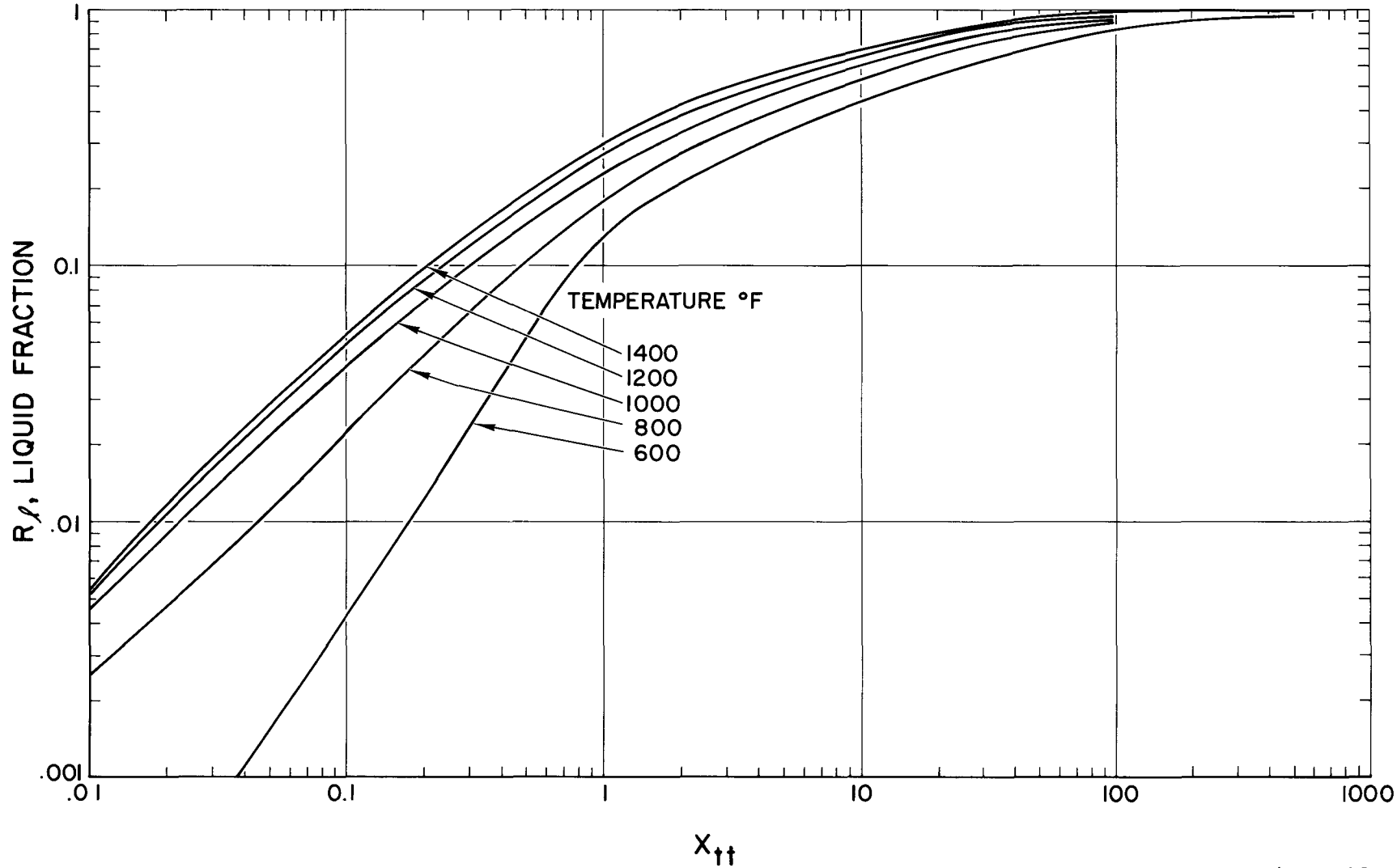

Figure 10. Liquid Fraction vs X_{tt} for Mercury

a given temperature, the vapor and liquid densities and viscosities were assumed to be constant through the boiling length.*

Figure 11 shows liquid fraction as a function of the relative location in the boiling length for exit qualities of 0.1, 0.3, 0.75, and 1, for boiling temperatures of 800 and 1400°F. The liquid fraction curves for 1000 and 1200°F lie intermediate to those shown in Figure 11. At 800°F boiling temperature the bulk of the liquid fraction distribution occurs in the initial portion of the boiling length. This is especially evident for an exit quality of 1 where about 90% of the total liquid fraction is concentrated in the first 25% of the boiling length. For lower exit qualities this trend is still in evidence but is less pronounced. As boiling temperature is increased, liquid fraction tends to be more uniformly distributed with greater liquid fraction extant at all points in the boiling length.**

The liquid fraction distributions for 800, 1000, 1200, and 1400°F were graphically integrated to obtain the length-average liquid fraction for the entire boiling section. Figure 12 shows the length-average liquid fraction as a function of exit quality and boiling temperature. The dashed curves below a quality of 0.1 are extrapolated. For an exit quality of 0.2, $\overline{R}_\ell$ increases from 0.096 to 0.352 by increasing the boiling temperature from 800 to 1400°F. For a boiling temperature of 1000°F, $\overline{R}_\ell$ increases from 0.06 to 0.27 when the exit quality decreases from 1 to 0.1. That is, a ten-fold reduction in exit quality results in only 4.5 times as great length-average liquid fraction.

---

* While in many cases the boiling pressure drop may be a substantial portion of the initial static pressure, the assumption of constant properties will not produce significant error in the prediction of liquid fraction. This is due to the condition that the bulk of the liquid fraction distribution occurs in the initial portion of the boiling length while the greatest portion of the boiling pressure drop occurs in the latter portion of the boiling length. Thus the greatest effect on property changes (gas density, primarily) occurs in the low liquid fraction distribution area. Of course, if the pressure distribution is known, the appropriate liquid fraction curves can be used.

** Note that all the liquid fraction curves for exit quality less than 1 are merely enlargements of a portion of the $x_o = 1$ curve. That is, the liquid fraction at the end of the boiling section $\left(\frac{z}{L} = 1\right)$ for an exit quality of 0.1, is the same as the liquid fraction at $\frac{z}{L} = 0.1$, for an exit quality of 1. A similar condition holds for the slip ratio curves shown in Figure 14.

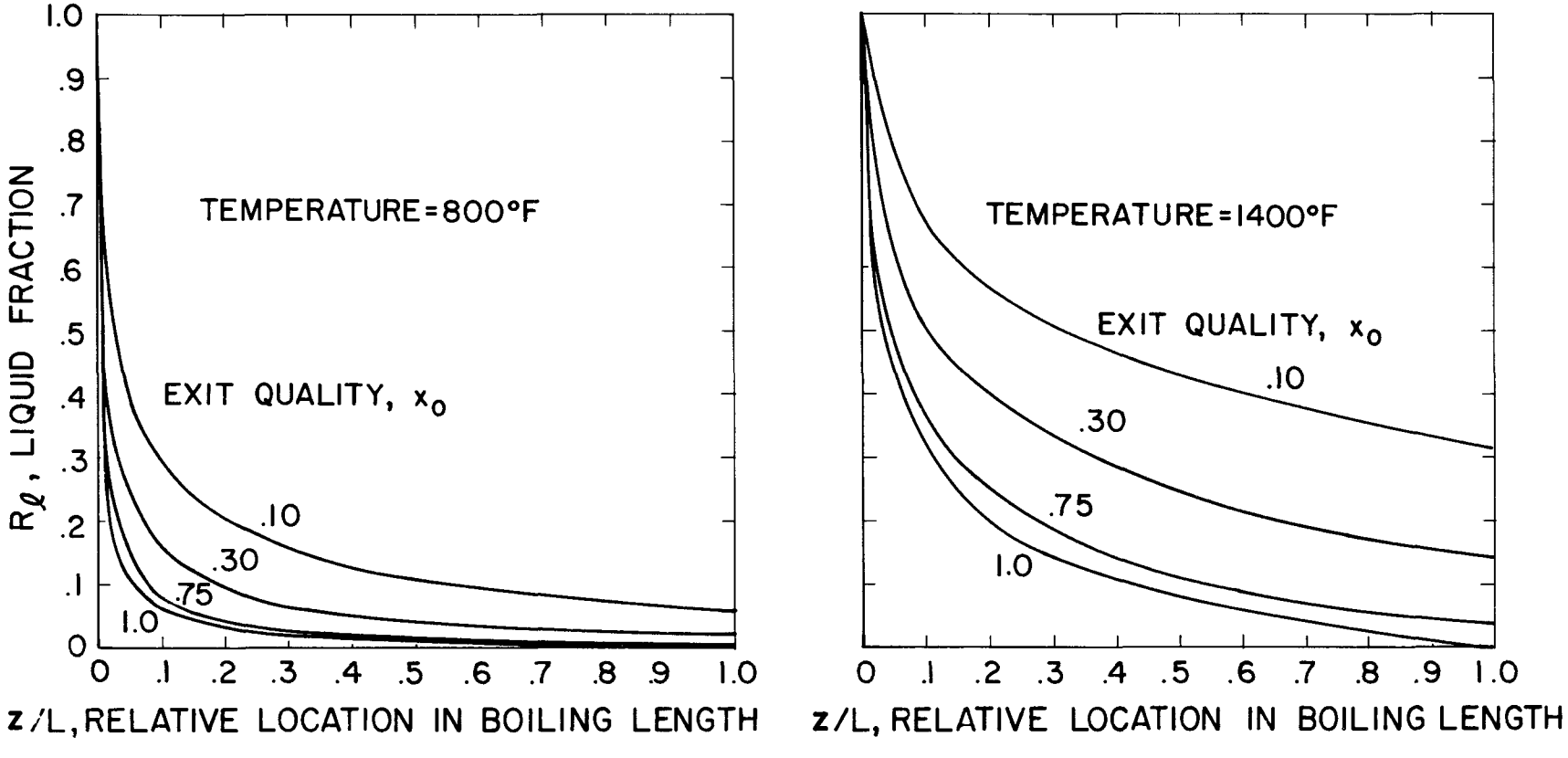

7569-0513

Figure 11. Liquid Fraction vs Relative Location in Boiling Length for Mercury With Uniform Heat Flux

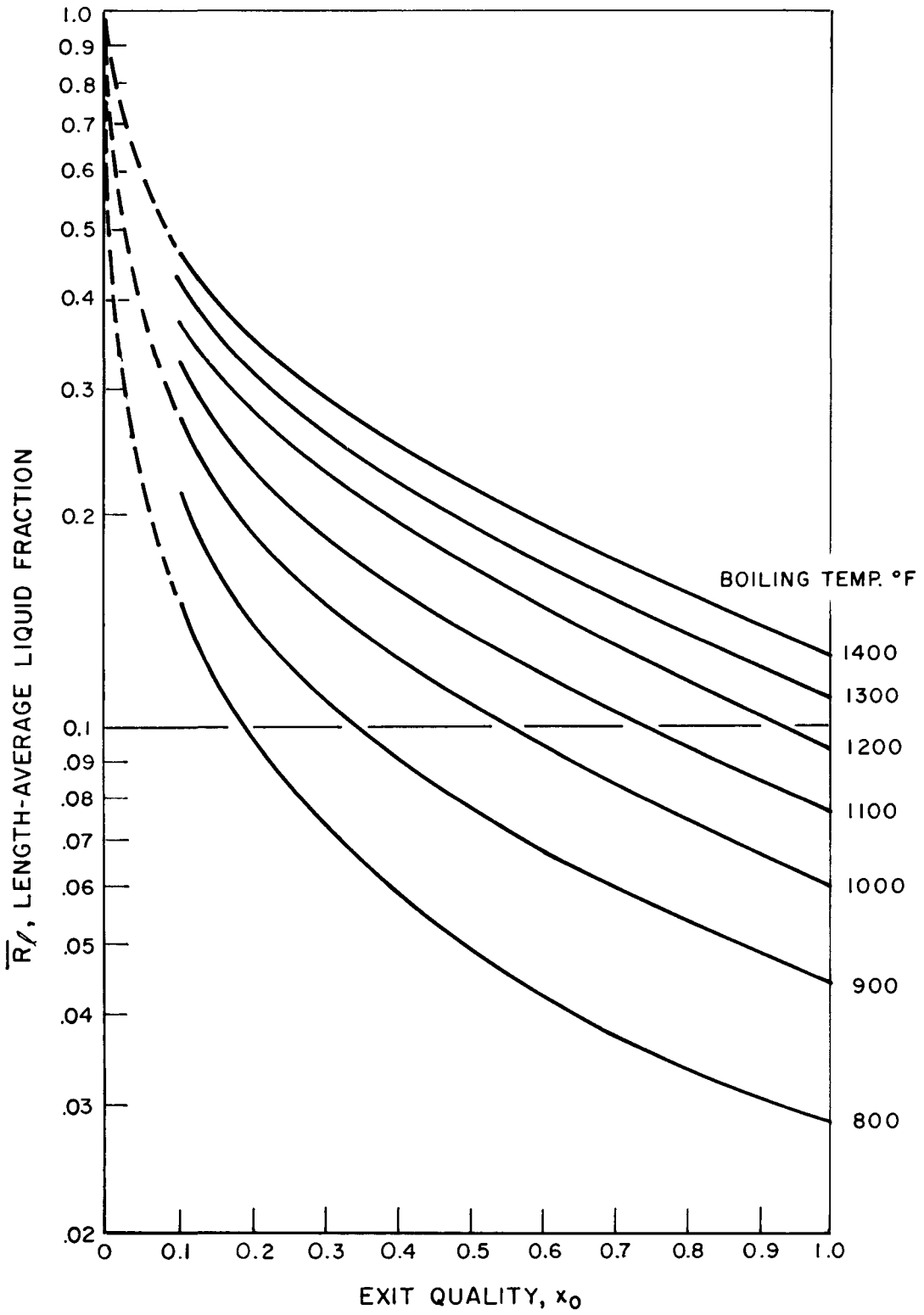

7569-0514

Figure 12. Length-Average Liquid Fraction vs Exit Quality for Boiling Mercury With Uniform Heat Flux

The length-average mixture density, $\overline{\rho}_m$, is expressed as

$$\overline{\rho}_m = \overline{R}_\ell \rho_\ell + (1 - \overline{R}_\ell)\rho_g \quad , \tag{8}$$

where $\overline{R}_\ell$ is the length-average liquid fraction, ρ_ℓ and ρ_g are the densities of the liquid and gas phases, respectively. Using the length-average liquid fraction information of Figure 12, the length-average mixture density was calculated by means of equation 8; the results are shown in Figure 13. For an exit quality of 0.2, the curves show that $\overline{\rho}_m$ increases rapidly* with boiling temperature going from 76 lb/cu ft, at 800°F, to 272 lb/cu ft at 1400°F. At 1000°F, $\overline{\rho}_m$ increases from 48 lb/cu ft to 210 lb/cu ft when the exit quality decreases from 1 to 0.1. That is, a ten-fold reduction in exit quality results in only 4.4 times as great length-average mixture density. This indicates that low-exit-quality boilers may offer advantages in weight reduction.

Consider a uniform heat flux forced convection mercury boiler which is to operate at 1200°F. From Figure 13, length-average mixture density, for an exit quality of 1, is 76 lb/cu ft; for an exit quality of 0.1, it is 285 lb/cu ft. If the average heat flux over the boiling length for the boiler with an exit quality of 1 is 10,000 BTU/hr ft^2, it may be assumed, because of nucleate boiling, that the average heat flux for the boiler with an exit quality of 0.1 will be about 100,000 BTU/hr ft^2. For a given vapor weight flow rate, the low-exit-quality boiler will thus require one-tenth the surface area of the high-exit-quality boiler. For equal tube size in each case, the required mercury inventory for the low-exit-quality boiler will be $\left(\frac{285}{76} \times \frac{1}{10}\right)$, or 37.5% of that required by the high-exit-quality boiler. An additional weight saving will be realized because of the decreased tube length of the low-exit-quality boiler. Of course, the low-exit-quality boiler requires a vapor-liquid separator, a return line, and a recirculating pump; the weight of these components may largely negate the mercury inventory weight saving. In an actual case, a complete system analysis is required for proper evaluation and comparison of the two systems.

* For exit qualities less than 0.1, the length-average mixture density approaches, and even exceeds, the density of commonly used tube materials.

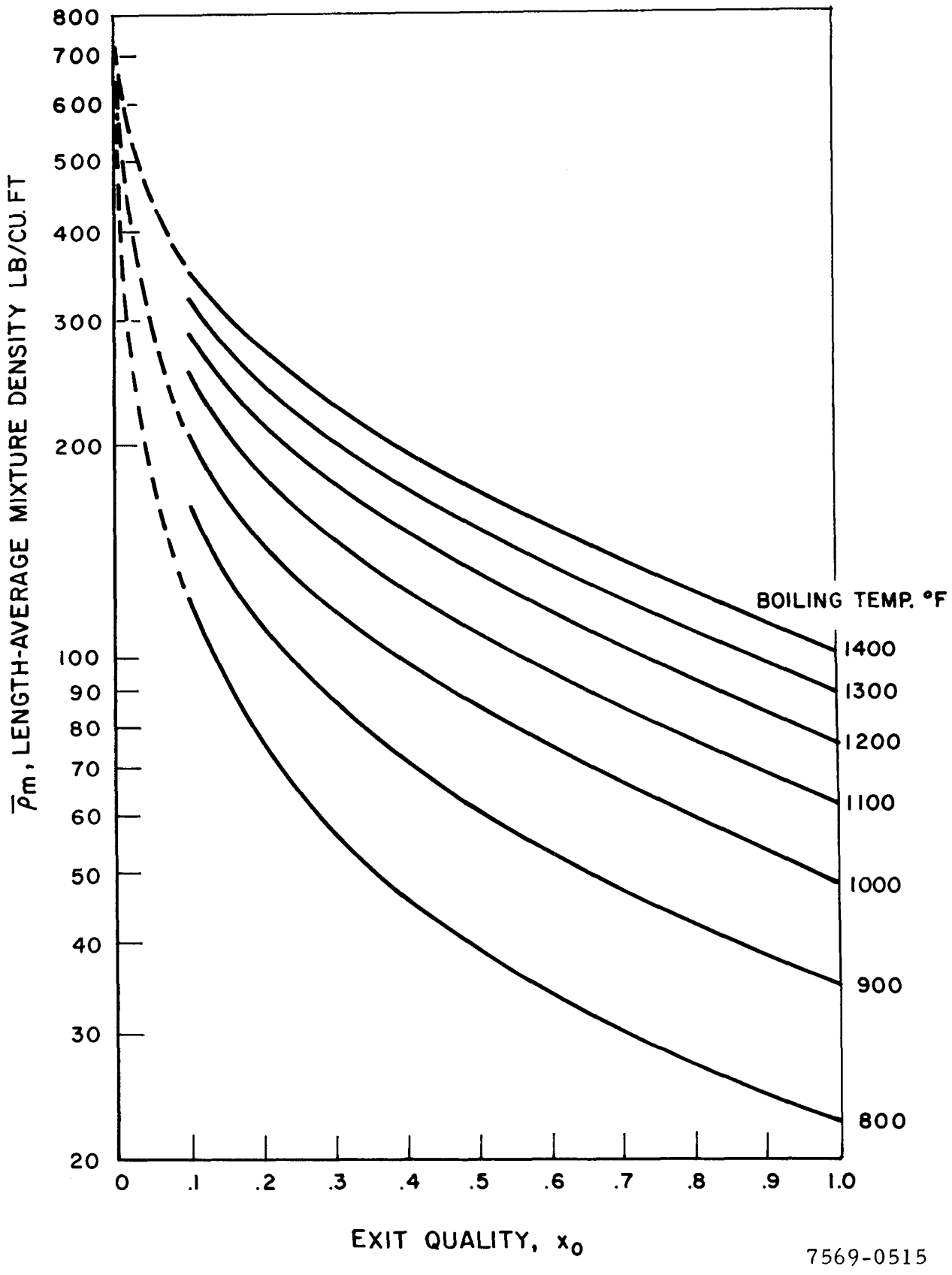

Figure 13. Length-Average Mixture Density vs Exit Quality for Boiling Mercury With Uniform Heat Flux

Figure 13 may also be used to determine the pressure difference, due to mixture gravity head, for a vertical boiler. This is especially important for determining the driving pressure in the case of a natural circulation boiler, but is also important in correcting boiling pressure-drop readings in a forced circulation, vertical boiler.

Utilizing the liquid fraction distribution computed previously (Figure 11) the slip ratio was calculated for exit qualities of 0.1, 0.3, and 0.75, and 1 for temperatures of 800, 1000, 1200, and 1400°F. The slip ratio, $\frac{V_g}{V_\ell}$, is defined as the ratio of gas velocity to liquid velocity in two-phase flow. The gas velocity is,

$$V_g = \frac{W_g}{\rho_g A (1 - R_\ell)} \quad , \tag{9}$$

where W_g is the gas flow rate, ρ_g is the gas density, A is the flow cross sectional area, and R_ℓ is the liquid fraction. Similarly, the liquid velocity is,

$$V_\ell = \frac{W_\ell}{\rho_\ell A R_\ell} \quad , \tag{10}$$

where W_ℓ is the liquid flow rate, and ρ_ℓ is the liquid density. Using the above equations the expression for slip ratio becomes,

$$\frac{V_g}{V_\ell} = \frac{W_g \rho_\ell R_\ell}{W_\ell \rho_g (1 - R_\ell)} \quad . \tag{11}$$

Figure 14 shows slip ratio as a function of relative location in the boiling length and exit quality, for boiling temperatures of 800, 1000, 1200, and 1400°F. Slip ratio increases very rapidly in the initial portion of the boiling length and thereafter increases at a slower rate. At 800°F, increasing exit quality from 0.1 to 0.75 increases the exit slip ratio from 8 to 12. At higher boiling temperatures the general trend is the same except for a more uniform increase in slip ratio and for lower slip ratios everywhere. The latter is the combined result of two

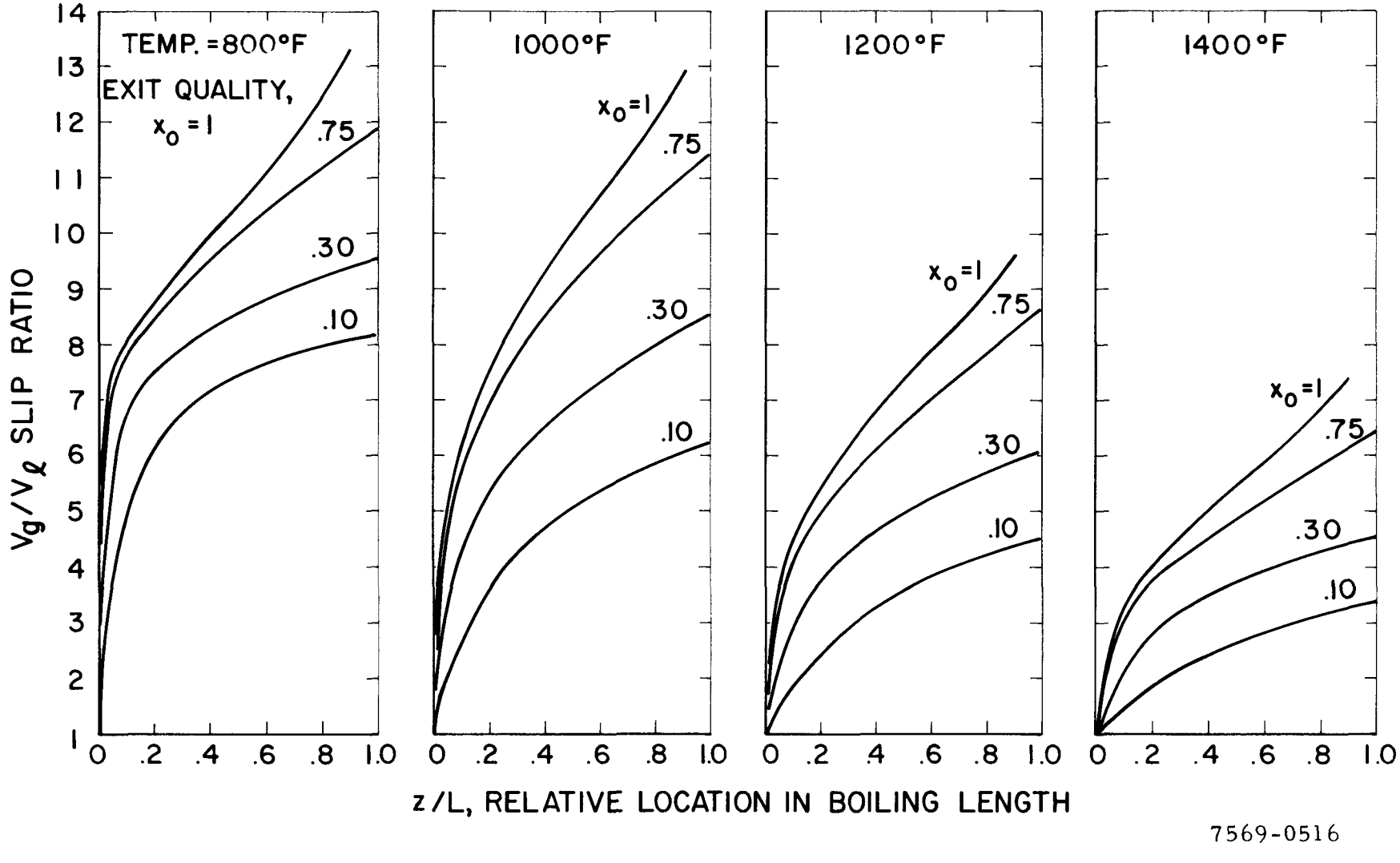

Figure 14. Slip Ratio vs Relative Location in Boiling Length for Mercury With Uniform Heat Flux

opposing influences: As boiling temperature increases for a given exit quality, $\frac{\rho_\ell}{\rho_g}$ decreases while $\frac{R_\ell}{1 - R_\ell}$ increases; the net result is a decrease in $\frac{V_g}{V_\ell}$. (See Equation 11.)

The generation of vapor during forced circulation boiling produces a substantial acceleration of the fluid stream. The change of momentum of the liquid and gas streams results in a pressure drop which is in addition to the friction pressure drop. The momentum pressure drop is usually a substantial portion of the overall boiling pressure drop except in the case of high length to diameter ratio boilers which produce dry vapor. This section describes the method by which the momentum pressure drop, for boiling mercury, may be determined.

The pressure drop resulting from the change of momentum of the fluid stream during boiling can be expressed[3] as,

$$(\Delta P)_M = \frac{1}{Ag}\left[W_T(1 - x_o)(V_\ell)_o + W_T(x_o)(V_g)_o - W_T(V_\ell)\right] \tag{12}$$

where $(\Delta P)_M$ is the momentum pressure drop, W_T is the total flow, x_o is the exit quality, A is the pipe flow cross-section, and V is velocity. The subscripts ℓ and g refer to the liquid and gas phases, respectively; the subscripts T and o refer to total and exit, respectively. Substitution of Equation 9 for $(V_g)_o$, and and Equation 10 for $(V_\ell)_o$ results in,

$$\Delta P_M = \frac{G_T^2}{g}\left(\frac{1}{\rho_\ell}\left[\frac{(1 - x_o)^2}{(R_\ell)_o} + \frac{\rho_\ell}{\rho_g}\,\frac{x_o^2}{1 - (R_\ell)_o} - 1\right]\right) \tag{13}$$

$$\Delta P_M = \frac{G_T^2}{g}\, r \tag{14}$$

where r corresponds to the terms contained in the parenthesis of Equation 13.

Equation 13 accounts for the different liquid and gas velocities and is the expression proposed by Martinelli-Nelson[3] for boiling water. The multiplier r, shown in Figure 15 was obtained by using the exit liquid fraction calculated previously (See Figure 11 at $z/L = 1$), for various exit qualities and by substituting the appropriate values into Equation 13. Figure 15 shows r as a function of mercury boiling temperature (800 to 1400°F) and exit quality ($x_o = 0.1$ to 1). Comparison with the r values of Martinelli-Nelson[3] for steam show that the present values are substantially less for identical values of ρ_ℓ/ρ_g. The primary reason for this is the much higher liquid density, ρ_ℓ, for mercury as compared to water.

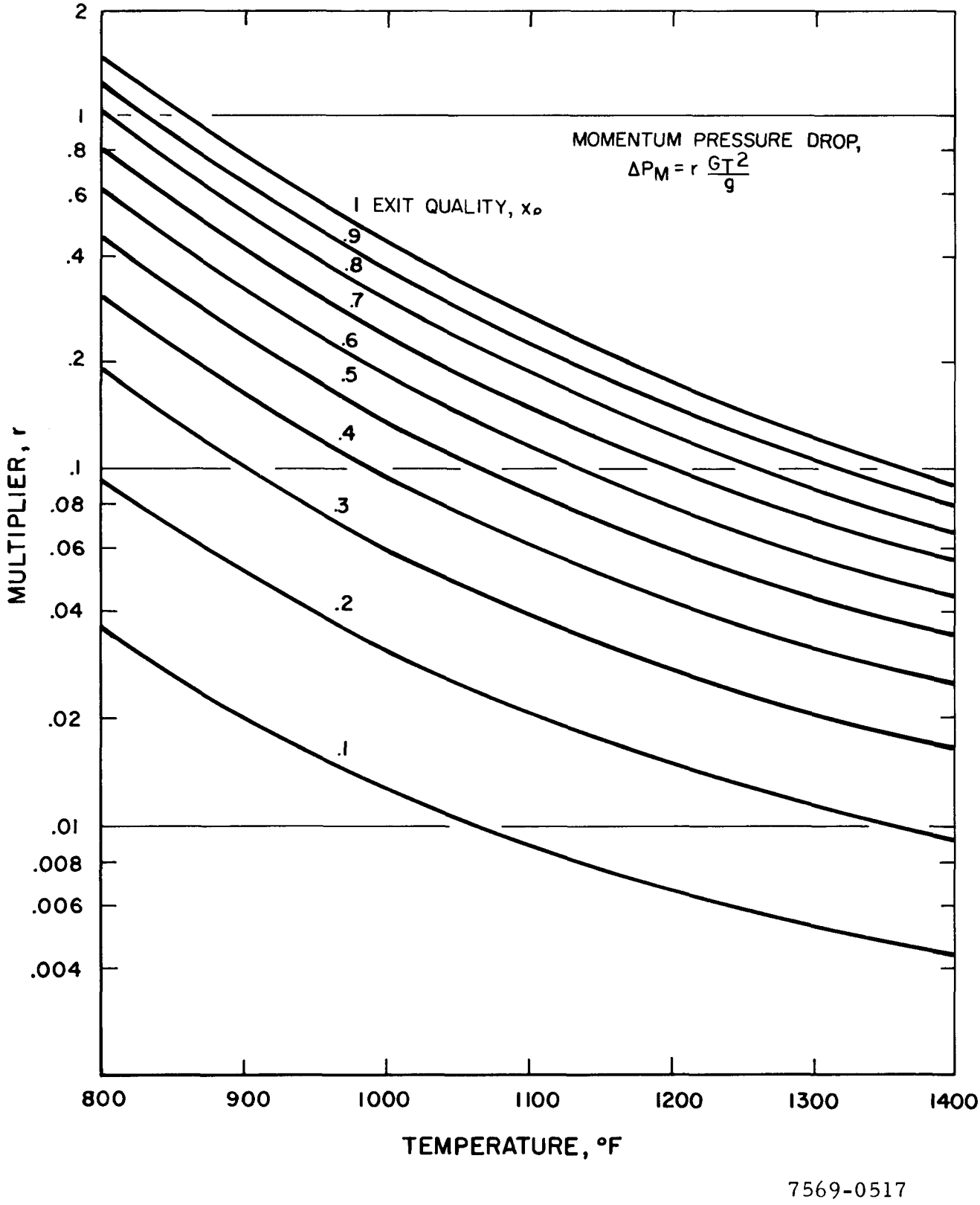

Figure 15. Multiplier r vs Temperature for Mercury

NOMENCLATURE

A_s = surface area of pipe, ft^2

A = cross sectional area of pipe, ft^2

C = constant in friction factor equation = 0.046 (turbulent flow); = 16 (viscous flow)

D = hydraulic diameter of pipe, ft

g = gravitational acceleration = 4.18×10^8 ft/hr^2

K = constant

L = total length of boiler, ft

G = mass velocity, lb/hr-sq ft

N_{R_g} = Reynolds number of gas based on pipe diameter = $G_g D/\mu_g$

N_{R_ℓ} = Reynolds number of liquid based on pipe diameter = $G_\ell D/\mu_\ell$

$(\Delta P/\Delta L)_g$ = pressure drop gradient due to gas flowing at rate W_g with a density ρ_g, lb/sq ft-ft

$(\Delta P/\Delta L)_\ell$ = pressure drop gradient due to liquid flowing at rate W_ℓ with a density ρ_ℓ, lb/sq ft-ft

$\Delta P/\Delta L$ = pressure drop gradient, lb/sq ft-ft

ΔP = pressure drop, lb/sq ft

P_w = wetted perimeter, ft

Q = heat transfer rate, btu/hr

r = momentum pressure drop multiplier = $\frac{1}{\rho_\ell}\left[\frac{(1 - x_o)^2}{R_{\ell_o}} + \left(\frac{\rho_\ell}{\rho_g}\right)\frac{x_o^2}{(1 - R_\ell)_o} - 1\right]$

R_g = fraction of pipe cross section occupied by gas = $1 - R_\ell$

R_ℓ = fraction of pipe cross section occupied by liquid

V = velocity, ft/hr

W_T = total weight flow (including gas and liquid), lb/hr

W_g = gas flow rate, lb/hr

W_ℓ = liquid flow rate, lb/hr

x = mixture quality = $W_g/(W_g + W_\ell)$

X_{tt} = two-phase flow modulus = $\left(\frac{W_\ell}{W_g}\right)^{0.9}\left(\frac{\rho_g}{\rho_\ell}\right)^{0.5}\left(\frac{\mu_\ell}{\mu_g}\right)^{0.1}$

X_{vt} = two-phase flow modulus = $\frac{1}{\left(N_{R_g}\right)^{0.4}}\left(\frac{C_\ell}{C_g}\,\frac{W_\ell}{W_g}\,\frac{\rho_g}{\rho_\ell}\,\frac{\mu_\ell}{\mu_g}\right)^{0.5}$

z = length along boiler, ft

ρ_g = density of gas, lb/cu ft

ρ_ℓ = density of liquid, lb/cu ft

μ_g = absolute viscosity of gas, lb/ft-hr

μ_ℓ = absolute viscosity of liquid, lb/ft-hr

λ = heat of vaporization, Btu/lb

SUBSCRIPTS

g = gas

ℓ = liquid

m = mixture

o = exit

t = turbulent

v = viscous

T = total

TP = two phase

tt = turbulent liquid-turbulent gas

vt = viscous liquid-turbulent gas

SUPERSCRIPTS

$-$ = average value, from integration over entire boiling length

REFERENCES

1. R. C. Martinelli, L. M. K. Boelter, T. H. M. Taylor, E. G. Thomsen, and E. H. Morrin, "Isothermal Pressure Drop for Two-Phase, Two-Component Flow in a Horizontal Pipe," Trans. ASME, 66, 1944, p. 139.

2. R. W. Lockhart and R. C. Martinelli, "Proposed Correlation of Data for Isothermal Two-Phase, Two-Component Flow in Pipes," Chemical Engineering Progress, 45, 1949, p. 39.

3. R. C. Martinelli and D. B. Nelson, "Prediction of Pressure Drop During Forced-Circulation Boiling of Water," Trans. ASME, 70, 1948, p. 695.

4. G. A. Hughmark and B. S. Pressburg, "Holdup and Pressure Drop With Gas-Liquid Flow in a Vertical Pipe," AIChE Journal, 7, no. 4, 1961, p. 677.

5. N. C. Sher, "Review of Martinelli-Nelson Pressure Drop Correlation," WAPD-TH-219, 1956.

6. S. G. Bankoff, "A Variable Density Single Fluid Model for Two-Phase Flow With Particular Reference to Steam-Water Flow," Journal of Heat Transfer, Trans. ASME, Series C, 82, 1960, p. 265.

7. S. Levy, "Prediction of Two-Phase Pressure Drop and Density Distribution From Mixing Length Theory," ASME paper 62-HT-6, 1962.

8. U. H. von Glahn, "An Empirical Relation for Prediction Void Fraction With Two-Phase, Steam-Water Flow," NASA TN D-1189, 1962.

9. R. Kiraly and A. Koestel, "The SNAP 2 Power Conversion System Topical Report No. 8, Condenser Development and Design Study," TRW Report No. ER-4104, June, 1960.

10. H. M. Dieckamp, R. Balent, and J. R. Wetch, "Compact Reactors for Space Power," Nucleonics, April, 1961, p. 73.

11. G. F. Hewitt, I. King, and P. C. Lovegrove, "Holdup and Pressure Drop Measurements in the Two-Phase Annular Flow of Air-Water Mixtures," AERE-R 3764, June, 1961.

12. G. F. Hewitt, I. King, and P. C. Lovegrove, "Techniques for Liquid Film and Pressure Drop Studies in Annular Two-Phase Flow," AERE-R 3921, March, 1962.

13. J. H. Vohr, "Flow Patterns of Two-Phase Flow - A Survey of Literature," TID-11514, Columbia University, December, 1960.

14. C. J. Baroczy and V. D. Sanders, "Pressure Drop for Flowing Vapors Condensing in a Straight Horizontal Tube," ASME paper 61-WA-257, 1961.

15. D. Chisholm and A. D. K. Laird, "Two-Phase Flow in Rough Tubes," Trans. ASME, 80, 1958, p. 276.

16. B. L. Richardson, "Some Problems in Horizontal Two-Phase, Two-Component Flow," ANL Report 5949, 1958.

17. W. D. Weatherford Jr., J. C. Tyler, and P. M. Ku, "Properties of Inorganic Energy Conversion and Heat Transfer Fluids for Space Applications," WADD Tech. Report 61-96, November, 1961.

18. H. S. Isbin, N. C. Sher, and K. C. Eddy, "Void Fractions in Two-Phase Steam-Water Flow," AIChE Journal, 3, No. 1, March 1957, p. 136.

19. H. C. Larson, "Void Fractions of Two-Phase Steam-Water Mixture," M. S. Thesis, University of Minnesota, 1957.

20. J. F. Marchaterre, "The Effect of Pressure on Boiling Density in Multiple Rectangular Channels," ANL Report 5522, February, 1956.

21. R. A. Egen, D. A. Dingee, and J. W. Chastain, "Vapor Formation and Behavior in Boiling Heat Transfer," BMI-1163, February, 1957.

22. F. Bergonzoli and F. J. Halfen, "Correlation of Void Fraction for Santowax R During Forced Circulation Boiling at Low Pressure," NAA-SR-TDR 7815, October, 1962.